Elongation of Fe–Fe atomic pairs in $Fe_{65}Ni_{35}$ Invar alloy determined by RMC method

Face-centered cubic (fcc) Fe–Ni alloys containing 35–36 at.% Ni are characterized by the Invar effect, which shows a nearly zero thermal expansion coefficient ($\alpha = 1.19 \times 10^{-6}$/K) within a wide temperature range up to the Curie temperature ($T_C \sim 505$ K). After the discovery of the Invar effect by Guillaume in 1897 [1], the macroscopic origin of this anomalous thermoelastic property has been interpreted as a cancellation of the thermal expansion by the shrinkage due to the magnetovolume effect. On the other hand, the atomic-scale origin of the large magnetovolume effect has not been understood thus far.

Since the zero thermal expansion of the lattice is related to the shallow curvature of the interatomic potential, the Invar alloy exhibits anomalously soft elastic properties under high pressures. The shallow interatomic potential has been interpreted theoretically as a 2γ-state model, in which two distinct spin states are hypothesized below T_C: a high-spin (HS) configuration associated with a large volume and a low-spin (LS) configuration with a small volume. More recent *ab initio* calculation results [2] indicated that the noncollinear spin alignment of Fe moments develops with increasing pressure, whereas Ni spin moments maintain linear spin alignments even under pressure, which also explains the elastic softening behavior in the Invar alloy. The element-dependent response of the magnetic structure under pressure motivated us to experimentally determine the local structures around Fe and Ni atoms separately.

This study focuses on the atomic-scale origin of the magnetovolume effects in Invar alloy [3]. The atomic arrangement in a model structure composed of 4000 Fe/Ni atoms was investigated using the reverse Monte Carlo (RMC) algorithm combined with complementary datasets of extended X-ray absorption fine structure (EXAFS) and X-ray diffraction (XRD) under high pressures. The pressure dependences of XRD and EXAFS were measured at SPring-8 **BL39XU** independently. Typically, it is difficult to distinguish the Fe and Ni atoms neighboring the X-ray absorbing atoms by conventional EXAFS analysis because of the small difference between the backscattering amplitudes of Fe and Ni. In contrast, the RMC method constructs an atomic cluster and finds the best atomic cluster model that matches the experimental EXAFS profiles at the Fe and Ni edges as well as the XRD patterns by trial-and-error iterations. Consequently, the length of each atomic pair can be evaluated from the determined cluster.

The RMC fits provided good agreement between the experimental and calculated profiles of the absolute values of Fourier transformed profiles ($|\mathrm{FT}[k^2\chi(k)]|$) at both the Fe and Ni edges of the Invar alloy (Fig. 1). The determined atomic cluster conserves the sequential stacks of (111) atomic planes, although much of the atoms are displaced from the ideal positions of the fcc lattice. Therefore, the RMC fits successfully visualize the structure of the alloy, where the local structure was largely distorted, although the disordered atomic cluster maintained the long-range periodicity to satisfy the Bragg law owing to the pseudo-fcc symmetry.

The partial pair distribution functions $g_{ij}(R)$ are determined from the atomic cluster and demonstrate the elongation of the first-nearest neighboring (1NN) Fe–Fe pairs in comparison with 1NN Fe–Ni and Ni–Ni pairs at 0.6 GPa (Fig. 2). As the pressure increases, the difference in $g_{ij}(R)$ profiles gradually decreases;

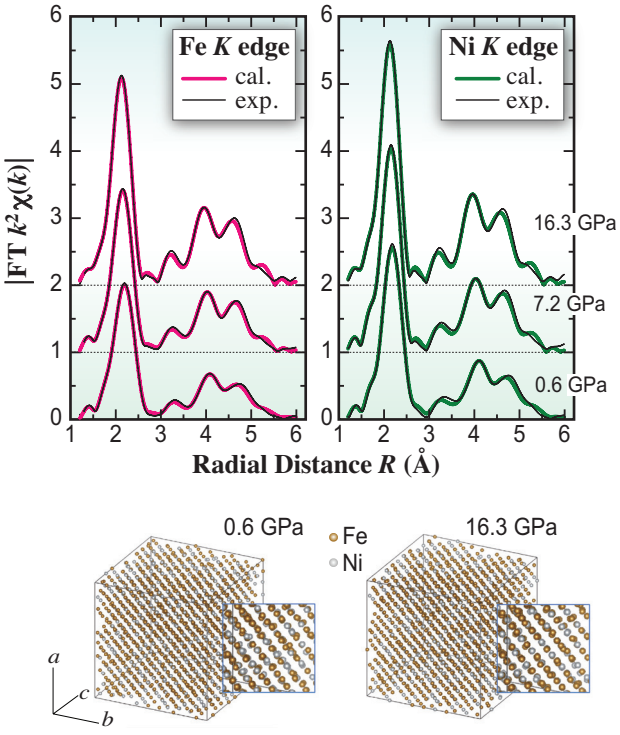

Fig. 1. Top: absolute values of Fourier transformed EXAFS profiles ($|\mathrm{FT}[k^2\chi(k)]|$) of $Fe_{65}Ni_{35}$ Invar at Fe and Ni *K*-edges. Bottom: atomic clusters of the Invar alloy obtained by the RMC method. The clusters viewed from the [11$\bar{2}$] direction are shown. The illustrations represent enlargements of the atomic cluster.

the profiles of these three pairs exhibit peaks at approximately the same position of $R \sim 2.455$ Å at 16.3 GPa. To highlight the elongation of Fe–Fe atomic pairs, the average lengths of the 1NN atomic pairs, R_{Fe-Fe}, R_{Fe-Ni}, and R_{Ni-Ni}, were quantitatively determined and are plotted in Fig. 3. Compared with R_{Fe-Ni} and R_{Ni-Ni}, the expansion of R_{Fe-Fe} is of the size of 0.02 Å at the lowest pressure of the Invar alloy (0.6 GPa). Because the Fe–Fe pairs are more compressive than others, the elongation of R_{Fe-Fe} decreases rapidly with increasing pressure; the evaluated R_{Fe-Fe} reaches the values of R_{Fe-Ni} and R_{Ni-Ni} at pressures above 10 GPa.

The Invar alloy undergoes a pressure-induced magnetic transition from the ferromagnetic phase to the paramagnetic phase at $P_c \sim 7$ GPa. The elongation and subsequent shrinkage of Fe–Fe pairs accompanied by the magnetic transition reveals that the volume changes owing to the magnetovolume effect originating mainly from the Fe–Fe pairs, while the lengths of Fe–Ni and Ni–Ni pairs seem to contribute less. Interestingly, the elongation of Fe–Fe pairs occurred also in the $Fe_{55}Ni_{45}$ non-Invar alloy [4], indicating that the existence of longer Fe–Fe pairs because of the magnetovolume effect is a common phenomenon in the Fe–Ni alloy with fcc symmetry. Because the $Fe_{55}Ni_{45}$ non-Invar alloy undergoes a pressure-induced Invar effect at ~7.5 GPa [4], we conclude that the delicate balance between the number of Fe–Fe pairs and their elongation depending on the magnetization play a crucial role in initiating the Invar effect. In this study, using the RMC method, we successfully demonstrated the feasibility of atomic-arrangement visualization for disordered alloys.

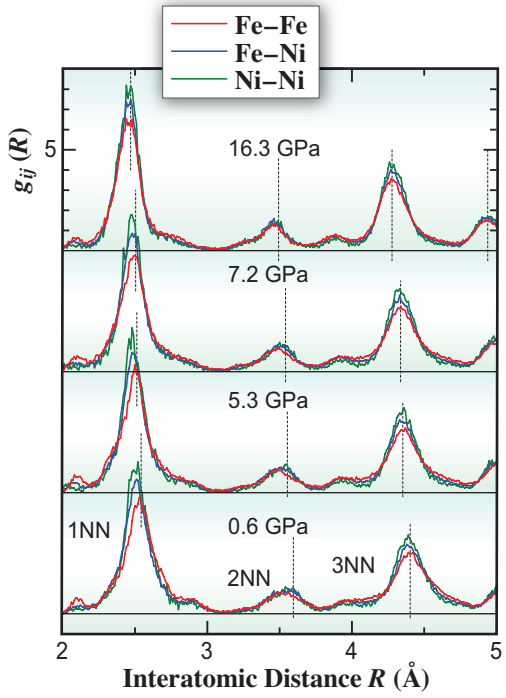

Fig. 2. Partial pair distribution functions $g_{ij}(R)$ of i and j atomic pairs up to third-nearest-neighboring (3NN) pairs, where i, j = Fe or Ni.

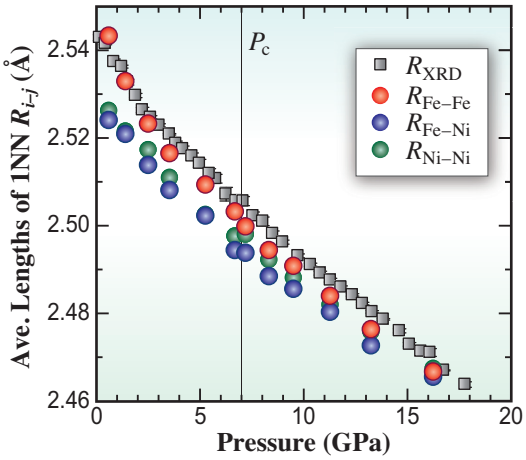

Fig. 3. Pressure dependences of the average length within a range of 0.6 Å centered on the 1NN peaks of Fe–Fe, Fe–Ni, and Ni–Ni pairs. Squares show average bond lengths determined from XRD.

Naoki Ishimatsu* and Naoto Kitamura

Division of Advanced Science and Engineering, Hiroshima University

*Email: ishimatsunaoki@hiroshima-u.ac.jp

References

[1] C. Guillaume and C.H. Seances: Acad. Sci. **125** (1897) 235 .
[2] M. van Schilfgaarde *et al.*: Nature **400** (1999) 46.
[3] *N. Ishimatsu, S. Iwasaki, M. Kousa, S. Kato, N. Nakajima, N. Kitamura, N. Kawamura, M. Mizumaki, S. Kakizawa, R. Nomura, T. Irifune, and H. Sumiya: Phys. Rev. B* ***103*** *(2021) L220102.*
[4] L. Dubrovinsky *et al.*: Phys. Rev. Lett. **86** (2001) 4851.